Partial Response CPM in Satellite Mobile Systems

John P. Fonseka and Xiao-Mei Yang

Abstract: **It is known that Gaussian minimum shift keying (GMSK) is an attractive signaling technique in mobile communications. In this study, it is demonstrated using partial response raised cosine (LRC) modulation that other partial-response continuous phase modulation (PR-CPM) techniques can perform better than GMSK in a mobile system.**

LRC signals are analyzed and compared with GMSK signals in a mobile channel. Differential phase detection (DPD) and limiter discriminator detection (LDD) receivers with decision feedback are separately considered for the detection of the two types of signals. In case of LRC signals, the delay of the DPD receiver, and the sampling instant of the LDD receiver are selected to minimize the error probability. Numerical results are presented for land mobile, satellite mobile and Gaussian channels at different bandwidths and Doppler shifts. It is shown that LRC signals can perform better than GMSK signals at the same bandwidth.

Index Terms: **LRC signals, GMSK signals, mobile channel, differential phase detection, limiter discriminator detection.**

I. INTRODUCTION

A satellite mobile channel (SMC) is defined as the channel between a satellite and a mobile vehicle. A SMC is generally characterized by the power ratio, K, the power of the direct signal component P_s to the power of the diffuse signal component P_d; $K = P_s/P_d$ [1]–[6]. The two limiting cases; $K = 0$ corresponds to a land mobile channel (LMC) with a Rayleigh envelope and uniformly distributed phase [7]–[11], while the case $k = \infty$ corresponds to a Gaussian channel. Typically for a SMC, K lies between 6 dB and 16 dB.

Due to the presence of nonlinear amplifiers and the strict bandwidth requirements, constant envelope modulation techniques such as partial response continuous phase modulation (PR-CPM) [12]–[14] techniques have been considered in satellite mobile communications [4]–[11]. Among PR-CPM techniques, Gaussian minimum shift keying (GMSK) has received considerable amount of attention due to its superior spectral properties [4]–[9], and it has been adopted as the signaling technique for the European GSM digital cellular system. Other PR-CPM signaling formats, such as tamed frequency modulation (TFM) [12] and generalized TFM (GTFM) [15], have also been considered over fading channels. For the detection of signals, non-coherent detection techniques such as differential phase detection (DPD) and limiter discriminator detection (LDD) are preferred over coherent detection techniques as it is difficult to recover the carrier phase in presence of a fading diffuse signal component. Hence, PR-CPM signaling with DPD or LDD are attractive choices of signaling over a SMC [4], [5]. In [17], it has been shown that the performance of GMSK signaling with DPD can be significantly improved in a Gaussian channel by using decision feedback (FB) to eliminate the effect of intersymbol interference (ISI) caused by previously decoded symbols. By using a similar approach, the performance of GMSK signals with DPD receiver and LDD receiver has been analyzed with and without FB in a SMC in [4] and [5], respectively along with a correction in [6].

So far, in the literature, PR-CPM formats with baseband pulses that are strictly limited to a finite duration have not been considered for signaling over a SMC. In this study, it is demonstrated that such PR-CPM signals with baseband pulses that are limited to a finite interval can perform better than GMSK signals. For demonstration, partial response raised cosine (PR-RC) signals are considered with LDD and DPD detection over a SMC, and compared with GMSK signals. The selection of the delay in the DPD receiver, and the sampling instant in LDD receiver are analyzed in detail. In the literature, full response raised cosine (FR-RC or, simply, 1RC) signals [12]–[14] have been considered in satellite mobile systems, and it has been shown that 1RC signals perform better than ordinary FSK signals in a SMC [17], [18]. However, the spectrum of 1RC signals, even though comparable with FSK signals, is considerably broader than that of GMSK signals. Hence, 1RC schemes cannot be reasonably compared with GMSK schemes. However, it is known that the spectral variations of PR-RC signals are similar to those of GMSK signals [12]–[14], and hence, PR-RC (or simply LRC) signals are comparable with GMSK signals. Numerical results presented here show that LRC signals can perform better than GMSK signals with DPD and LDD receivers in a SMC at the same bandwidth. The two types of signals, GMSK and LRC, are compared at different bandwidths, different Doppler shifts, and different values of K. In order to achieve better performance, receivers with feedback are considered with both types of signals. LRC signals with different lengths of the baseband pulse are considered.

II. SYSTEM DESCRIPTION

A PR-CPM signal corresponding to any transmitted binary information sequence $\boldsymbol{a} = (\cdots, a_{-1}, a_0, a_1, \cdots)$; $a_i \in \{+1, -1\}$ takes the form [4]

$$\begin{aligned} x(t, \boldsymbol{a}) &= \sqrt{2P_s}\exp[j\pi h \int_{-\infty}^{t} \sum_{i=-\infty}^{\infty} a_i g(\tau - iT)d\tau] \\ &= \sqrt{2P_s}\exp[j\phi(t, \boldsymbol{a})], \end{aligned} \quad (1)$$

Manuscript received January 7, 1999; approved for publication by Yong-Hwan Lee, Division I Editor, August 4, 2000.

The authors are with School of Electrical Engineering and Computer Science The University of Texas at Dallas, EC33 2601 N. Floyd Road Richardson, Texas 75080 U.S.A.

where P_s is the average signal power, T is the bit duration, h is the modulation index, and $\phi(t, \boldsymbol{a})$ is the phase variation due to information. The quantity $g(t)$ is the baseband frequency pulse and for RC signals $g(t)$ takes the form [12]

$$g(t) = \begin{cases} [1 - \cos(2\pi t/LT)]/(LT), & 0 \le t < LT \\ 0, & \text{otherwise}, \end{cases} \quad (2)$$

while for GMSK signals it is the response of a Gaussian filter to a rectangular pulse which can be written as [4]

$$g(t) = [Q(cB_tT(-t/T)) - Q(cB_tT(1 - t/T))]/T, \quad (3)$$

where $c = 7.546$, B_tT is the normalized bandwidth of the Gaussian filter, and $Q(\cdot)$ is the standard Q function. RC signals with $g(t)$ given by (2) are referred to as LRC signals, and signals with $L > 1$, those considered in this study, form the class of PR-RC signals. The modulation index of GMSK signals is set at $h = 0.5$, while it is considered as a variable for LRC signals.

After passing over the SMC, the received signal can be written as [4]

$$r_i(t, \boldsymbol{a}) = s(t, \boldsymbol{a}) + d(t, \boldsymbol{a}) + n_i(t), \quad (4)$$

where

$$\begin{aligned} s(t, \boldsymbol{a}) &= \sqrt{2P_s}\exp[j(\phi(t, \boldsymbol{a}) + 2\pi f_D t)] \\ &= \sqrt{2P_s}\exp[j\phi_s(t, \boldsymbol{a})] \end{aligned} \quad (5)$$

is the direct component,

$$d(t, \boldsymbol{a}) = \sqrt{P_d}\exp[j\phi(t - t_d, \boldsymbol{a})]\xi(t), \quad K = P_s/P_d \quad (6)$$

is the diffuse component, $n_i(t)$ is additive white Gaussian noise with two-sided power spectral density $N_0/2$, f_D is the Doppler shift of the direct component, and $\phi_S(t, \boldsymbol{a})$ is the total phase variation of the direct component. Further, P_d is the power of the diffuse signal, t_d is the delay of the diffuse component with respect to the direct component, and $\xi(t)$ is a zero mean Gaussian process with autocorrelation [4]

$$R_\xi(\tau) = J_0(2\pi f_{Dm}\tau), \quad (7)$$

where $J_0(\cdot)$ is the zero-order Bessel function of the first kind, and f_{Dm} is the maximum Doppler frequency. The quantities f_{Dm} and f_D are generally normalized with respect to the signaling rate as

$$F_{Dm} = f_{Dm}T, \quad F_D = f_DT. \quad (8)$$

Fig. 1 shows the block diagram of non-coherent detection with FB of LRC signals. The received signal $r_i(t, \boldsymbol{a})$ is first passed through a receiver front-end filter to remove out-of-band noise. The front-end filter is assumed to have sufficient bandwidth to pass the signal without causing any distortion, specifically, the noise bandwidth B_n of it is assumed to be the 99% bandwidth of the transmitted signal. This assumption has been commonly made in the literature with GMSK signals [4], [5]. Since, the spectral roll-off of GMSK and LRC signals are similar to each other [12]–[14], the same assumption is made here

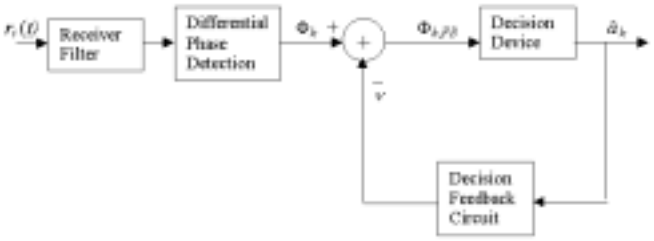

Fig. 1. Non-coherent detection with decision feedback.

with LRC signals. Hence, the signal used for detection can be written in the form [4]

$$\begin{aligned} r(t, \boldsymbol{a}) &= s(t, \boldsymbol{a}) + d(t, \boldsymbol{a}) + n(t) \\ &= s(t, \boldsymbol{a}) + \mu(t, \boldsymbol{a}), \end{aligned} \quad (9)$$

where $n(t)$ is the filtered noise signal with power N_0B_nT, and $\mu(t, \boldsymbol{a}) = d(t, \boldsymbol{a}) + n(t)$. The signal to noise ratio of the receiver is the ratio of the total received signal power ($P_s + P_d$) to the noise power P_n;

$$SNR = (P_s + P_d)/P_n = E_b/(N_0B_nT), \quad (10)$$

where $E_b = (P_s + P_d)T$ is the bit energy. The phase angle of the filtered signal $\phi_r(t, \boldsymbol{a})$, which is used for detection can be expressed as [4]

$$\phi_r(t, \boldsymbol{a}) = \phi_s(t, \boldsymbol{a}) + \eta(t, \boldsymbol{a}), \quad (11)$$

where

$$\eta(t, \boldsymbol{a}) = \tan^{-1}\frac{\mu'_Q(t, \boldsymbol{a})}{\sqrt{2\rho} + \mu'_I(t, \boldsymbol{a})}, \quad (12)$$

$$\begin{aligned} \mu'(t, \boldsymbol{a}) &= \mu'_I(t, \boldsymbol{a}) + j\mu'_Q(t, \boldsymbol{a}) \\ &= \mu(t, \boldsymbol{a})\exp[-j\phi_s(t, \boldsymbol{a})], \end{aligned} \quad (13)$$

and

$$\begin{aligned} \rho &= P_s/(P_d + P_n) = \Gamma K/(1 + \Gamma), \\ \Gamma &= P_d/P_n = SNR/(1 + K). \end{aligned} \quad (14)$$

III. DPD WITH FB OF LRC SIGNALS

Since $g(t)$ is non-zero only between 0 and LT, the decision variable corresponding to any symbol a_k is derived by observing the phase variation $\phi_r(t, \boldsymbol{a})$ starting from $t = kT$ as

$$\begin{aligned} \Phi_k &= \phi_r(kT + t_0, \boldsymbol{a}) - \phi_r(kT, \boldsymbol{a}) \\ &= \phi_k + W_Dt_n + \eta_k, \end{aligned} \quad (15)$$

where $t_n = t_0/T$, t_0 is the delay in the DPD, W_Dt_n represents the Doppler shift, $\eta_k = [\eta(kT + t_0) - \eta(kT)]$ represents the differential phase noise, and $W_D = 2\pi F_D$. The term ϕ_k represents the contribution from the message symbols which can be

Table 1. Values of θ_i (in degrees) of *L*RC signals.

L	θ_0	θ_1	θ_2	θ_3	θ_4
2	90	90	·	·	·
3	35.19	109.62	35.19	·	·
4	16.35	73.65	73.65	16.35	·
5	8.75	46.41	69.68	46.41	8.75

written as

$$\phi_k = \pi h a_k \int_0^{t_0} g(t)dt + \pi h \sum_{i=1}^{L-1} a_{k-i} \int_0^{t_0} g(t+iT)dt + \pi h \sum_{i=1}^{L'} a_{k+i} \int_0^{t_0} g(t-iT)dt, \quad (16)$$

where $L' = \lfloor t_0/T \rfloor$, $\lfloor x \rfloor$ and denotes the largest integer not greater than x. It is noticed that the first term in (16) is the desired term which is dependent only on a_k, while the second and third terms represent the intersymbol interference (ISI) from previous and future symbols, respectively. Further, the integrals in (16) can be written as

$$\pi \int_0^{t_0} g(t)dt = \sum_{j=0}^{L'-1} \theta_j + \beta_{L'}, \quad (17)$$

where

$$\theta_j = \pi \int_{jT}^{(j+1)T} g(t)dt; \quad j = 0, 1, \cdots, (L-1), \quad (18)$$

$$\beta_l = \pi \int_{lT}^{(lT+t_\alpha)} g(t)dt; \quad l = 0, 1, \cdots, (L-1), \quad (19)$$

and $t_\alpha = t_0 - L'T$. Table 1 lists the values of of θ_j all *L*RC signals considered in this study, $L = 2$ through 5, while the values of β_l, which are dependent on t_α, can be calculated according to (19). The feedback loop calculates the interference caused by previously decoded symbols, $\hat{a}_{k-i}$, as

$$\nu = \pi h \sum_{i=1}^{L-1} a_{k-i} \int_0^{t_0} g(t+iT)\, dt, \quad (20)$$

and deducts it from the output of the DPD (see Fig. 1). As in other studies [4], [5], assuming that the previously decoded symbols are correct, i.e., $\hat{a}_{k-i} = a_{k-i}$, $i = 1, \cdots, L-1$, the decision variable with feedback can be written as

$$\begin{aligned} \Phi_{k,FB} &= \Phi_k - \nu \\ &= \pi h a_k \int_0^{t_0} g(t)\, dt + \pi h \sum_{i=1}^{L'} a_{k+i} \int_0^{t_0} g(t-iT)\, dt \\ &\quad + W_D t_n + \eta_k \\ &= \phi_{k,FB} + W_D t_n + \eta_k, \end{aligned} \quad (21)$$

where

$$\phi_{k,FB} = \pi h a_k \int_0^{t_0} g(t)\, dt + \pi h \sum_{i=1}^{L'} a_{k+i} \int_0^{t_0} g(t-iT)dt. \quad (22)$$

Since the phase difference of the transmitted signal is positive (between 0 and π) and negative (between $-\pi$ and 0) for the two symbols $a_k = +1$ and $a_k = -1$, respectively, the DPD with FB receiver of *L*RC signals discussed here uses the decision rule:

$$\begin{aligned} a_k &= -1, \quad \text{if} \quad -\pi \le \Phi_{k,FB} < 0, \\ a_k &= +1, \quad \text{if} \quad 0 \le \Phi_{k,FB} < \pi, \end{aligned} \quad (23)$$

at every value of L, which is identical to that of 1-bit DPD of GMSK signals [4].

The selection of t_0 is an important decision in DPD of *L*RC signals, and it has to be selected to achieve good performance while maintaining a simple receiver structure. In case of GMSK signals, the highest phase variation due to any transmitted symbol occurs during that interval, and hence, $t_0 = T$ is optimal for GMSK signals with the above decision rule. However, in case of *L*RC signals, the highest phase variation occurs around the middle of the baseband pulse which can occur during any succeeding interval depending on the value of L, and hence, t_0 also needs to be selected depending on the value of L. It follows from (16) and (17) that the desired term can be maximized by choosing $t_0 = LT$, however, that will also introduce $(L-1)$ number of non-zero interfering future symbols. On the other hand, the interference from future symbols can be totally eliminated by choosing $t_0 = T$, which will, however, reduce the desired term. Hence, t_0 has to be selected by jointly considering the desired term with the interference terms. Therefore, the optimal t_0 needs to be calculated by averaging over all possible ISI terms, and hence, it cannot be expressed in closed form. However, it is known that the performance in presence of ISI is generally dominated by the worst case sequence that produces the value of the decision variable closest to a decision boundary [19]. Hence, the optimal value of t_0, at lower values of h, can be approximately calculated by finding the time instant that maximizes $\phi_{k,FB}$ corresponding to the worst case sequence; $a_k = +1$ and $a_{k+i} = -1$ for all $i > 0$. It is mentioned here that according to the decision rule in (23), at lower values of h, the error probability is dominated by decisions associated with the boundary at 0, while at higher values of h, it is dominated by those associated with the boundary at $\pm\pi$ [19]. However, since lower values of h are considered here to limit the bandwidth of the signals, the worst case sequence would be that corresponding to $a_k = +1$ and $a_{k+i} = -1$ for all $i > 0$. Fig. 2 shows the variation of $\phi_{k,FB}$ in (22) with t_0 of all *L*RC signals considered here corresponding to the worst case sequence. It is seen from Fig. 2 that at any value of L, an approximate optimal delay t_0 can be selected to maximize $\phi_{k,FB}$ corresponding to the worst case sequence. Table 2 lists these values of t_0 of all *L*RC signals, found by examining the variations in Fig. 2. The exact optimal values that minimizes the error probability which depends on the channel and the value of h can be calculated by searching around the approximate optimal t_0 values listed in Table 2. However, it was numerically found that the exact optimal

Table 2. Optimum values of t_0 obtained using the worst case sequence and the values of t_0 as multiples of $T/2$ used in the analysis.

L	t_0/T optimal	t_0/T used
2	1.5	1.5
3	2	2
4	2.41	2, 2.5
5	2.73	2, 2.5, 3

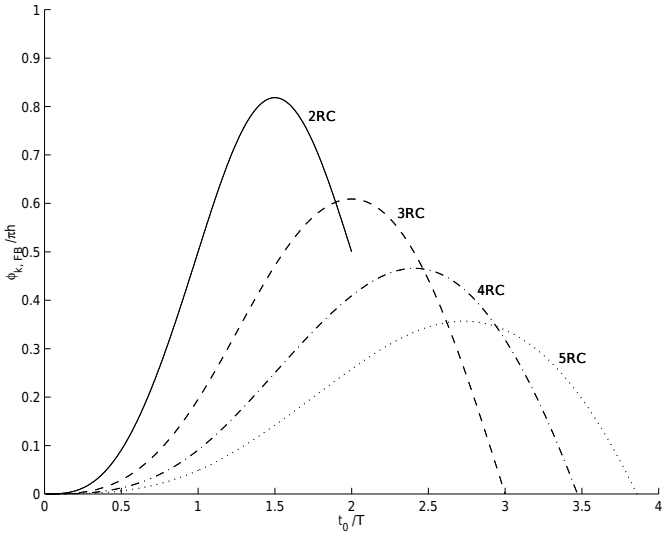

Fig. 2. Variation of $\phi_{k,FB}$ with t_0 of DPD of LRC signals corresponding to the worst case sequence.

values of t_0 are very close to that found by using the worst case sequence, and the degradation caused by selecting a value of t_0 close to the exact optimal value is negligible in all cases considered here. However, since t_0 has to be extracted from symbol timing information, the complexity of the resulting receiver can be significantly reduced by selecting a value of t_0 as a multiple of $T/2$. Hence, all DPD receivers considered in this study employ a delay equal to a multiple of $T/2$, and Table 2 lists the selected values of t_0 for the schemes considered in this study along with the approximate optimal values.

The error probability calculation of the DPD receiver in a satellite mobile channel in presence of ISI has been well documented in [4], [6]. The error probabilities of the DPD receiver of LRC, and GMSK signals with 1-bit ($t_n = 1$) and 2-bit ($t_n = 2$) DPD with feedback are also computed using the same method. It is recalled here that GMSK signals with 1-bit DPD uses the same decision rule as that of LRC signals. However, GMSK with 2-bit DPD uses differential encoding to form the transmitted sequence $\boldsymbol{a}$ from the message sequence $\boldsymbol{b}$, and employs the following decision rule; $b_k = -1$ if $-\delta \leq \Phi_{k,FB} < \delta$, and $b_k = +1$ if $\delta \leq \Phi_{k,FB} < (2\pi - \delta)$ [4]. Further, the value of δ depends on the channel, Doppler shift, and also the signal to noise ratio. Hence, comparing with 2-bit DPD of GMSK signals, DPD of LRC signals discussed here have a considerably simpler decision rule.

IV. LDD WITH FB OF LRC SIGNALS

The decision variable of the LDD receiver corresponding to any symbol a_k is the derivative of the phase variation $\phi_r(t, \boldsymbol{a})$ at time $t = kT + t_a$ as [5]

$$\begin{aligned} w_k &= \dot{\phi}_r(kT + t_a, \boldsymbol{a}) \\ &= \dot{\phi}_s(kT + t_a, \boldsymbol{a}) + w_D + \dot{\eta}_k(kT + t_a, \boldsymbol{a}) \\ &= w_{ks} + w_D + \dot{\eta}_k, \end{aligned} \tag{24}$$

where $w_{ks} = \dot{\phi}_s(kT + t_a, \boldsymbol{a})$ is the contribution to the decision variable by the message symbols, $w_D = 2\pi f_D$ is the contribution due to the Doppler shift, and $\dot{\eta}_k = \dot{\eta}_k(kT + t_a, \boldsymbol{a})$. The contribution from the message symbols can be written as

$$\begin{aligned} w_{ks} &= \pi h a_k g(t_a) + \pi h \sum_{i=1}^{L-1} a_{k-i} g(t_a + iT) \\ &\quad + \pi h \sum_{i=1}^{L'} a_{k+i} g(t_a - iT), \end{aligned} \tag{25}$$

where, $L' = \lfloor t_a/T \rfloor$. As with DPD of LRC signals, it is noticed that the first term in (26) is the desired term which is dependent only on a_k, while the second and third terms represent interference from previous and future symbols, respectively. As with the DPD receiver, assuming that the previously decoded symbols are correct, the decision variable with feedback can be written as

$$\begin{aligned} w_{k,FB} &= \pi h a_k g(t_a) + \pi h \sum_{i=1}^{L'} a_{k+i} g(t_a - iT) \\ &\quad + w_D + \dot{\eta}_k \\ &= w_{ks,FB} + w_D + \dot{\eta}_k, \end{aligned} \tag{26}$$

where

$$w_{ks,FB} = \pi h a_k g(t_a) + \pi h \sum_{i=1}^{L'} a_{k+i} g(t_a - iT). \tag{27}$$

Since the derivative of the phase of the transmitted symbol is positive and negative for the two symbols $a_k = +1$ and $a_k = -1$, respectively, the decision rule of the LDD with FB receiver of LRC signals, at every value of L, is:

$$\begin{aligned} a_k &= +1, \quad \text{if} \quad w_{k,FB} \geq 0, \\ a_k &= -1, \quad \text{if} \quad w_{k,FB} < 0, \end{aligned} \tag{28}$$

which is identical to that of LDD of GMSK signals [5].

Similar to t_0 in DPD, the value of t_a in LDD is selected to achieve good performance without complicating the receiver too much. It follows from (2) and (27) that when $L = 2$, the desired term can be maximized by choosing $t_a = T$ without introducing any interference. Hence, when $L = 2$, $t_a = T$ is the best choice of the sampling instant. Further, when $L = 2$ and $t_a = T$, it is seen from (25) and (27) that the amount fed back is zero, and hence, the receiver discussed here can be simplified for 2RC signals by removing the feedback loop. However, when $L > 2$, as with the selection of t_0 in the DPD receiver, t_a has to be selected by jointly considering the desired term with the interference terms. It is recalled that the highest rate of phase variation due to any transmitted symbol of GMSK signals occurs

Table 3. Optimum values of t_a obtained using the worst case sequence.

L	2	3	4	5
$t_a = T$	1	1.25	1.5	1.75

Table 4. Optimum h and t_0, and the corresponding $B_{99}T$ when $F_{Dm} = F_D = 0$.

L	t_0/T	$K=0$		$K=10$		$K=\infty$	
		h	$B_{99}T$	h	$B_{99}T$	h	$B_{99}T$
2	1.5	0.49	1.03	0.52	1.06	0.53	1.07
3	2.0	0.53	0.92	0.59	0.98	0.61	0.99
4	2.5	0.58	0.86	0.62	0.90	0.66	0.95
5	3.0	0.60	0.82	0.67	0.88	0.68	0.89

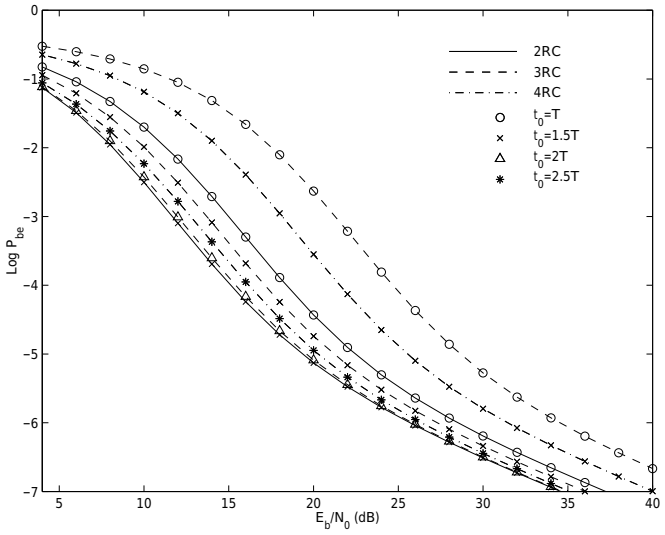

Fig. 3. Bit error probability variations of DPD of 2RC, 3RC and 4RC signals with optimal h in a SMC with $K = 10$ and $F_{Dm} = F_D = 0$.

at the middle of that interval, and hence, $t_a = T/2$ is optimal for GMSK signals. As with the calculation of t_0 of DPD, optimal t_a of the LDD can be approximately calculated by finding the time instant that maximizes $w_{ks,FB}$ in (27) corresponding to the worst case sequence; $a_k = +1$ and $a_{k+1} = -1$ for all $i > 0$. Table 3 lists these approximate optimal values of t_a of all LRC signals found from the variations of $w_{ks,FB}$ with t. As with DPD, it was numerically found that the exact optimal values of t_a are very close to those found by using the worst case sequence. Since the values of t_a listed in Table 3 are already multiples of $T/4$ (simple multiples of T), they are directly used in numerical results. The error probability of the LDD receiver is calculated by following the analysis in [5] with the correction stated in [6].

V. NUMERICAL RESULTS AND DISCUSSION

The error probability variations of DPD and LDD of LRC signals are compared with those of GMSK signals in Gaussian and mobile channels assuming the delay between the direct and diffuse components $t_d = 0$. Figs. 3–7 show the numerical results of the DPD receiver. The error probability variation of LRC signals with h is first presented. Recalling that $\phi_{k,FB}$ in (22) is proportional to h, one can expect an optimal value of h to minimize the overall error probability according to the decision rule

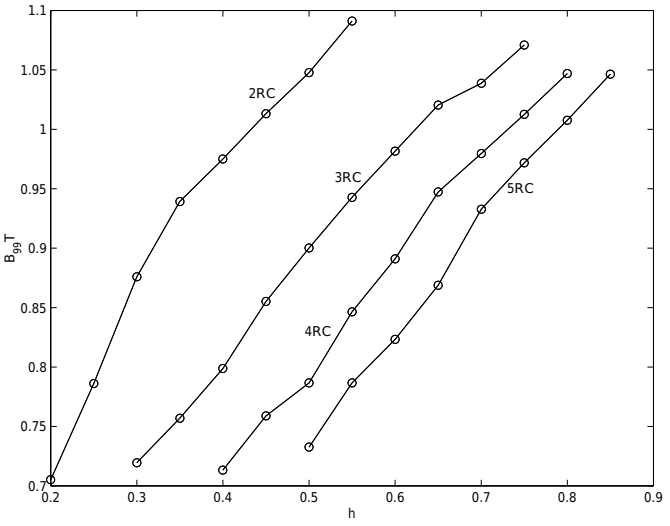

Fig. 4. Variation of the 99% bandwidth of LRC signals with h.

given by (23). Since the bandwidth increases with h, schemes that operate at modulation indices higher than these optimal values are not considered here since they occupy wider bandwidths and yet produce higher error probabilities. Table 4 lists optimal values of h and the best values of t_0 as multiples of $T/2$, to minimize the overall error probability at $E_b/N_0 = 24$ dB, when $K = 0$, 10, and ∞, and $F_{Dm} = F_D = 0$, along with the corresponding 99% bandwidth of the signals. Fig. 3 shows the error probability variations of LRC signals at these optimal values of h in a SMC with $K = 10$, and $F_{Dm} = F_D = 0$ for $L = 2$ through 4. In order to demonstrate the sensitivity to the delay in DPD, variations corresponding to different delays have been plotted in Fig. 3. At these optimal values of h, the overall optimal delays were numerically found to be, $t_0 = 1.47T$ for 2RC signals, $t_0 = 1.89T$ for 3RC signals, $t_0 = 2.35T$ for 4RC signals, and $t_0 = 2.74T$ for 5RC signals. It is seen that these optimal values are close to those listed in Table 2 which were found by using the worst case sequence. Further, the error probability variations at these optimal delays are very close to those of 2RC with $t_0 = 1.5T$, 3RC with $t_0 = 2T$, 4RC with $t_0 = 2.5T$, and 5RC with $t_0 = 3T$ (not shown in Fig. 3) respectively. These variations are so close to each other that one can hardly notice a difference when plotted together, and hence, only the variations with t_0 values at multiples of $T/2$ are plotted in Fig. 3. It is seen from Fig. 3 that the receivers are significantly less sensitive to the delay t_0 close to its optimal value, but the sensitivity increases as the value of t_0 moves away from the optimal value. It is also seen that all LRC schemes with the best delay have similar error probability variations, however, as seen from Table 4, the bandwidth at higher values of L is lower than that at lower values of L.

Let us now compare the performance of LRC signals with DPD with those of GMSK signals with 1-bit and 2-bit DPD at similar bandwidths. Comparisons are made with the GMSK schemes discussed in [4], and hence, modulation indices of LRC signals are selected to produce similar bandwidths. To demonstrate the variation of bandwidth with h, Fig. 4 shows the variation of the 99% bandwidth of LRC signals with h for $L = 2$

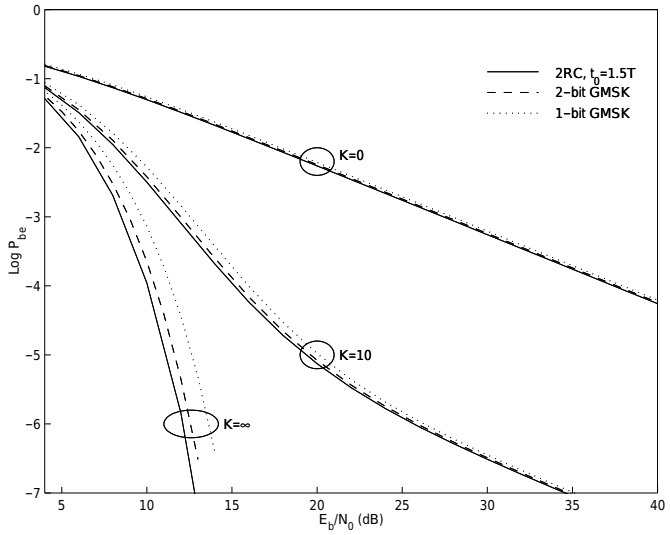

Fig. 5. Bit error probability variations of DPD of 2RC signals with $h = 0.5$ and GMSK signals with $B_tT = 0.5$, when $K = 0$, 10, and ∞, and $F_{Dm} = F_D = 0$.

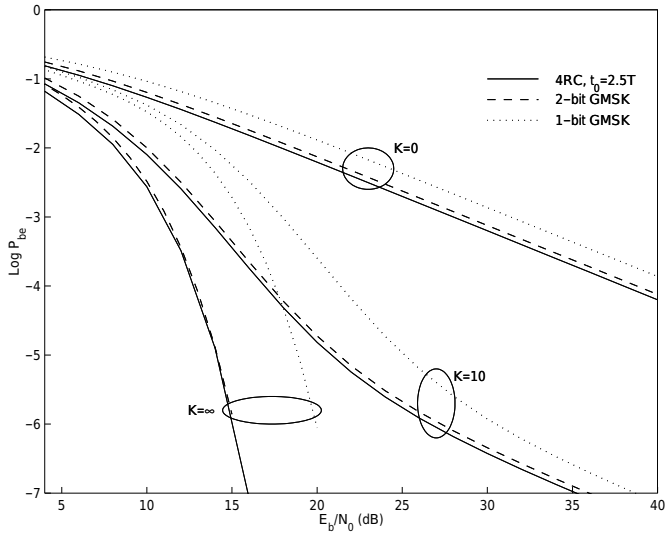

Fig. 6. Bit error probability variations of DPD of 4RC signals with $h = 0.5$ and GMSK signals with $B_tT = 0.2$, when $K = 0$, 10, and ∞, and $F_{Dm} = F_D = 0$.

Table 5. LRC schemes selected for comparison with GMSK schemes.

	Compared with GMSK with $B_tT = 0.5$, $B_{99}T = 1.04$		Compared with GMSK with $B_tT = 0.25$, $B_{99}T = 0.86$		Compared with GMSK with $B_tT = 0.2$, $B_{99}T = 0.79$	
L	h	$B_{99}T$	h	$B_{99}T$	h	$B_{99}T$
2	0.5	1.04	0.3	0.87	0.25	0.78
3	0.7	1.03	0.45	0.85	0.4	0.79
4	0.8	1.04	0.55	0.84	0.5	0.78
5	0.85	1.04	0.65	0.86	0.55	0.78

through 5. In order to compare with the GMSK schemes in [4], signals at three different bandwidths, $B_{99}T \approx 1.04$, $B_{99}T \approx 0.86$, and $B_{99}T \approx 0.79$ are considered here. Table 5 lists the selected modulation indices (as multiples of 0.05) of LRC signals and their corresponding bandwidths for comparison with each GMSK signal considered in [4]. Fig. 5 shows the bit error probability variation of 2RC signals with $h = 0.5$, when $K = 0$, 10, and ∞, and $F_{Dm} = F_D = 0$. It was found that, at this bandwidth $B_{99}T \approx 1.04$, 2RC signals perform best among all LRC signals listed in Table 5. For comparison, the error probability variations of GMSK signals with 1-bit and 2-bit DPD are also plotted in Fig. 5. Similarly, Fig. 6 shows the bit error probability variation of the best LRC signal when $B_{99}T \approx 0.79$ along with the corresponding variations of GMSK signals, when $K = 0$, 10, and ∞, and $F_{Dm} = F_D = 0$. It is seen from Fig. 5 and Fig. 6 that LRC signals perform better than GMSK signals. Further, as stated before, the decision rule of 2-bit DPD of GMSK signals is more complicated than that of LRC signals. In order to demonstrate the effect of a Doppler shift, Fig. 7 shows the error probability variation of the two best LRC schemes along with those of GMSK schemes when $B_{99}T \approx= 0.86$ in a SMC with $K = 10$ when $F_D = F_{Dm} = 0.01$, and in a LMC when $F_{Dm} = 0.01$. It is noted here that in a LMC ($P_s = 0$), the parameter F_D does not exist due to the absence of a direct component in (4). It is seen from Fig. 7 that LRC signals perform better than GMSK signals even in presence of a Doppler shift.

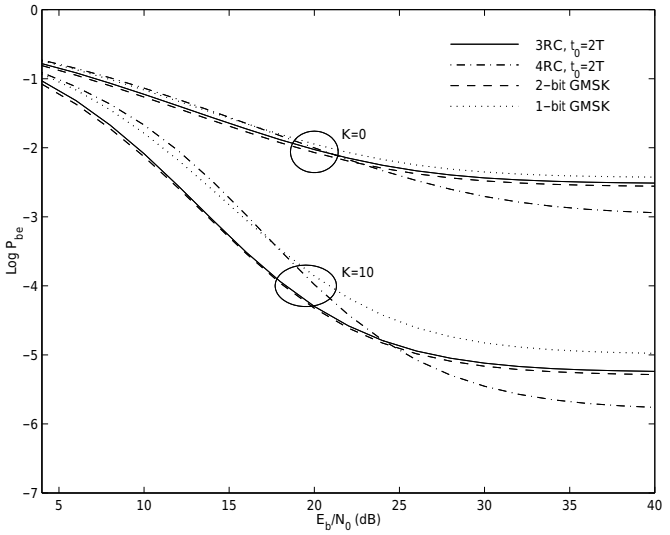

Fig. 7. Bit error probability variations of DPD of 3RC signals with $h = 0.45$, 4RC signals with $h = 0.55$ and GMSK signals with $B_tT = 0.25$, in a SMC with $K = 10$ and $F_{Dm} = F_D = 0.01$, and in a LMC with $F_{Dm} = 0.01$.

Similarly, Figs. 8–10 show the numerical results of the LDD receiver. It was numerically found that among all LRC signals that have been considered here, 2RC and 3RC signals perform better than 4RC and 5RC signals in all cases considered here. For illustration, Fig. 8 shows the error probability variations of LRC signals along with that of GMSK signals in a satellite mobile channel with $K = 10$, when $F_{Dm} = F_D = 0$, at $B_{99}T \approx= 0.86$. It is noticed that 2RC and 3RC signals perform close to each other and perform significantly better than 4RC and 5RC signals. Hence, the remaining numerical results of the LDD receiver are presented only for 2RC and 3RC signals. It was numerically found that the overall optimal values of t_a that minimizes the error probabilities in Fig. 8 at $E_b/N_0 = 24$ dB are; $t_a = T$ for 2RC signals, $t_a = 1.33T$ for 3RC signals, $t_a = 1.57T$ for 4RC signals, and $t_a = 1.79T$ for 5RC signals. It is mentioned that the overall optimal value of t_a of 2RC signals

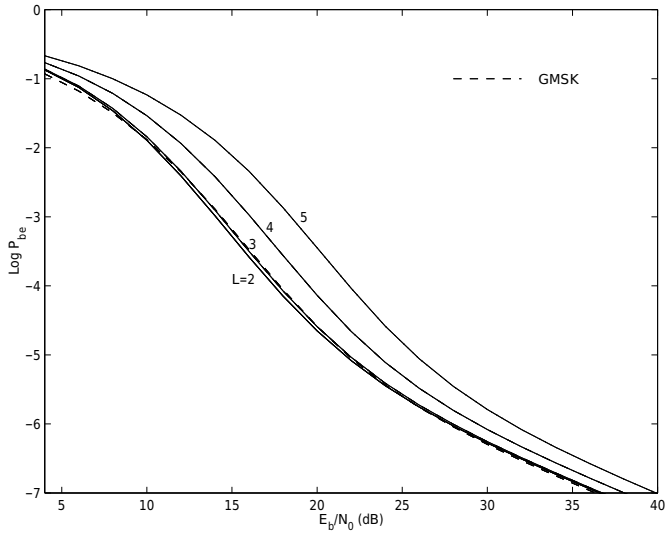

Fig. 8. Bit error probability variations of LDD of LRC and GMSK signals with $B_tT = 0.25$ in a SMC with $K = 10$, when $F_{Dm} = F_D = 0$.

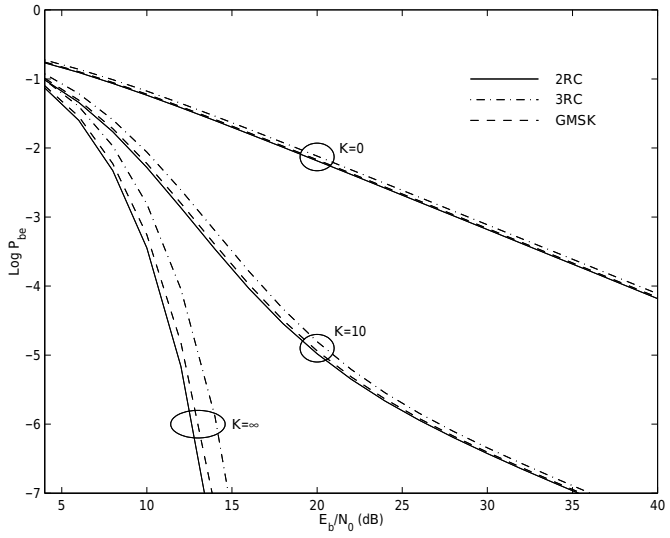

Fig. 9. Bit error probability variations of LDD of 2RC signals with $h = 0.25$, 3RC signals with $h = 0.4$, and GMSK signals with $B_tT = 0.2$ when $K = 0$, 10, and ∞, and $F_{Dm} = F_D = 0$.

is always T, and hence, all 2RC schemes that are considered here are optimal with respect to t_a, when $t_d = 0$. It is seen that even when $L > 2$, the optimal values are close to those listed in Table 3 which were found by using the worst case sequence. As with DPD, it was further found that the error probability variations at these optimal values of t_a are very close to those at values of t_a listed in Table 3, and hence, only the variations with t_a values listed in Table 3 are plotted in Fig. 8 and in the remaining figures. Fig. 9 shows the bit error probability variations of 2RC with $h = 0.25$ and 3RC signals with $h = 0.4$, along with the corresponding variation of GMSK signals, at $B_{99}T \approx 0.79$, when $K = 0$, 10, and ∞, and $F_{Dm} = F_D = 0$. It is seen from Fig. 9 that 2RC signals perform better than GMSK and 3RC signals. Fig. 10 demonstrates the effect of a Doppler shift by plotting the error probability variations of 2RC, 3RC, and GMSK signals, at $B_{99}T \approx 0.79$, in a SMC with $K = 10$, when

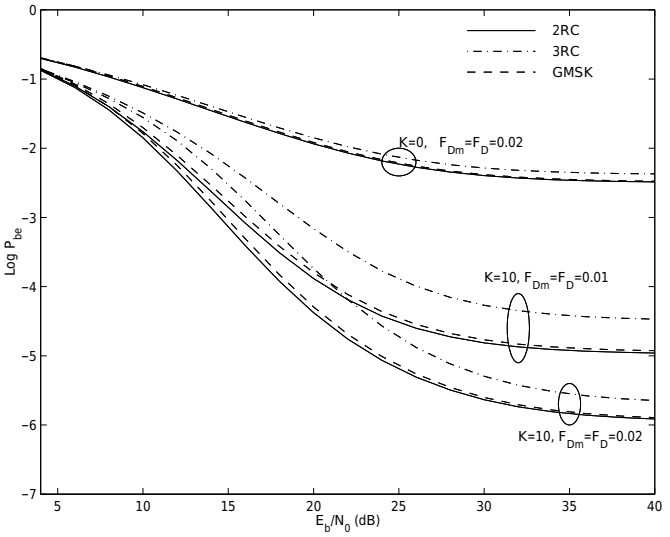

Fig. 10. Bit error probability variations of LDD of 2RC signals with $h = 0.25$, 3RC signals with $h = 0.4$ and GMSK signals with $B_tT = 0.2$, in a SMC with $K = 10$ and $F_{Dm} = F_D = 0.01$ and 0.02, and in a LMC with $F_{Dm} = 0.02$.

$F_{Dm} = F_D = 0.1$ and 0.2, and in a LMC when $F_{Dm} = 0.02$. As with DPD, it is seen from Fig. 10 that LRC signals can perform better than GMSK signals both in presence and in absence of a Doppler shift with LDD too.

It is noticed that at higher bandwidths, LRC signals with lower values of L perform better, and as the bandwidth decreases, higher values of L tend to perform better. It is seen from the numerical results that in case of DPD, different values of L perform best depending on the situation. However, in case of LDD, it is also noticed that, at all bandwidths considered here, 2RC signals perform best among all LRC signals. Further, as it has been stated before, LDD of 2RC signals does not require a feedback loop, and the sampling instant $t_a = T$, can be directly taken from the symbol timing information.

Even though only PR-RC signals have been considered here, one can similarly compute the error probabilities with other forms of partial response signals with baseband pulses such as half cycle sinusoid (HCS), spectral raised cosine (SRC), etc., which produce spectral variations similar to GMSK signals. The optimal delays and optimal modulation indices will however, depend on the baseband pulse. In case of LDD detection, it is noticed that when $L = 2$, signals can be detected without any interference, regardless of the pulse shape, and the optimal sampling instant remains at $t_a = T$.

VI. CONCLUSIONS

It has been demonstrated using LRC signals that other forms of CPM signals can perform better than GMSK signals in a mobile channel. LRC and GMSK signals have been analyzed and compared in a satellite mobile channel with DPD and LDD receivers with decision feedback. In case of DPD, the delay in the differential phase detector, and in case of LDD, the sampling instant of the discriminator have been selected to minimize the error probability. The bit error probabilities of LRC signals are presented along with those of GMSK signals, in land mobile,

satellite mobile, and Gaussian channels, at different bandwidths and Doppler shifts. It has been shown that both DPD and LDD of *L*RC signals perform better than GMSK signals.

REFERENCES

[1] F. Davarian, "Channel simulation to facilitate mobile satellite communication research," *IEEE Trans. Commun.*, vol. 35, pp. 47–56, Jan. 1987.

[2] L. J. Mason, "Error probability evaluation for systems employing differential detection in a Rician fast fading environment and Gaussian noise," *IEEE Trans. Commun.*, vol. 35, pp. 39–46, Jan. 1987.

[3] I. Korn and M. Namet, "M-ary frequency shift keying with differential phase detector in satellite mobile channel with narrowband receiver filter," *IEE Proc.-I*, vol. 137, pp. 33–37, Feb. 1990.

[4] I. Korn, "GMSK with differential phase detection in satellite mobile channel," *IEEE Trans. Commun.*, vol. 38, pp. 1980–1986, Nov. 1990.

[5] I. Korn, "GMSK with limiter discriminator detection in satellite mobile channel," *IEEE Trans. Commun.*, vol. 39, pp. 94–101, Jan. 1991.

[6] I. Korn, "Correction to GMSK with differential phase detection in the satellite mobile channel," *IEEE Trans. Commun.*, vol. 43, pp. 1264, Feb./Mar./Apr. 1995.

[7] S. M. Elnoubi, "Analysis of GMSK with discriminator detection in land mobile radio channels," *IEEE Trans. Veh. Tech.*, vol. 35, pp. 71–76, May 1986.

[8] F. Adachi and K. Ohino, "Performance analysis of GMSK frequency detection with decision feedback in digital land mobile radio," *IEE Proc.-F*, vol. 135, pp. 199–207, June 1988.

[9] M. K. Simon and C. C. Wang, "Differential detection of Gaussian MSK in mobile radio environment," *IEEE Trans. Veh. Tech.*, vol. 33, pp. 307–320, Nov. 1984.

[10] K. S. Chung, "Generalized tamed frequency modulation and its application for mobile radio communications," *IEEE Trans. Veh. Tech.*, vol. 33, pp. 103–113, Aug. 1984.

[11] V. K. Kumar and S. C. Gupta, "Partial response continuous phase modulation and DPCM coding for speech transmission in cellular mobile radio systems," *IEEE Trans. Veh. Tech.*, vol. 35, pp. 100–105, Aug. 1986.

[12] C.-E. Sundberg, "Continuous phase modulation," *IEEE Commun. Mag.*, vol. 24, pp. 25–38, Apr. 1986.

[13] T. Aulin, N. Rydbeck, and C.-E. Sundberg, "Continuous phase modulation-part II: Partial response signaling," *IEEE Trans. Commun.*, vol. 29, pp. 210–225, 1981.

[14] J. B. Anderson, T. Aulin, and C.-E. Sundberg, *Digital Phase Modulation*, Plennum Press, 1986.

[15] K. S. Chung, "Generalized tamed frequency modulation and its application for mobile radio communications," *IEEE Trans. Veh. Tech.*, vol. 33, pp. 103–113, 1984.

[16] A. Yongacoglu, D. Marakis, and K. Feher, "Differential detection of GMSK using decision feedback," *IEEE Trans Commun.*, vol. 36, pp. 641–649, June 1988.

[17] J. P. Fonseka, "Baseband pulse shaping to improve narrowband FSK in satellite mobile systems," *IEEE Trans. Veh. Tech.*, vol. 41, pp. 724–729, Nov. 1992.

[18] I. Korn, "The effect of pulse shaping and transmitter filter on the performance of FSK-DPD and CPM-DPD in satellite mobile channel," *IEEE J. Select. Areas Commun.*, vol. 13, pp. 245–249, Feb. 1995.

[19] J. P. Fonseka, "Improved decision boundaries of narrowband M-ary CPFSK," *IEEE Trans. Commun.*, vol. 42, pp. 2204–2207, June 1994.

John P. Fonseka was born in Negombo, Sri Lanka. He has received the Ph.D. degree in Electrical Engineering from the Arizona State University in 1988.

He joined the University of Texas at Dallas in August of 1988, where he is currently an Associate Professor in Electrical Engineering. His research interests include combined coded modulation, signaling through bandlimited channels, coding theory, information theory, satellite mobile communications, telecommunication networks, and coherent optical communications.

Xiao-Mei Yang received a Master degree in electrical engineering from the University of Texas at Dallas in 1999. She joined the Nanjing Electronic Device Institute in 1992. Currently, she is working with the Nextel Communications of Texas engaged in frequency planning.